Electronic Supplementary Material (ESI) for Journal of Materials Chemistry C

Supporting Information

Effect of the molecular weight of the polymer gate dielectric on the performances of solution-processed ambipolar OTFTs

By Appan Merari Masillamani, Emanuele Orgiu, Paolo Samorì

Contents:

1. Surface free energy

The surface free energy of the polymeric dielectrics and organic semiconductor was estimated from the Owens and Wendt method.[1]

The contact angle with Millipore water, ethylene glycol and dimethyl sulfoxide (DMSO) was first measured on the thin films of polymer dielectrics or organic semiconductor spin casted from solution on Si/SiO_2 substrates by means of a Krüss DSA100 (drop shape analysis system) goniometer. The resulting contact angle values were utilized in the equation s1 to estimate the dispersive and polar components, from which the resulting sum of the dispersive and polar components gave the total surface free energy of the organic semiconductor (F8BT) and the polymeric dielectric (PMMA and PS) films.

$$\frac{\sigma_L(1+\cos\theta)}{2\sqrt{\sigma_L^D}} = \sqrt{\sigma_S^P}\frac{\sqrt{\sigma_L^P}}{\sqrt{\sigma_L^D}} + \sqrt{\sigma_S^D} \qquad \textbf{(s1)}$$

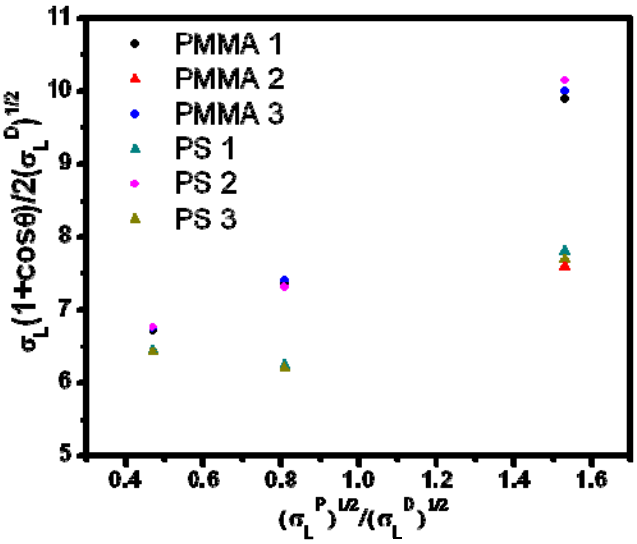

Figure S1. Plot of contact angle of the three different solvents with the surface of the polymeric dielectrics and the ratio the square root of the polar and dispersive components.

Note that the equation s1 is of the form y= mx+ c (the equation of a straight line) hence from the Figure s1 the polar component of the solid surface energy i.e., the component due to dipolar can be estimated the slope of the line and dispersive component can be extracted from the intercept

with the y-axis. The total surface free energy of the thin films can be estimated by taking the sum of dispersive and polar components.

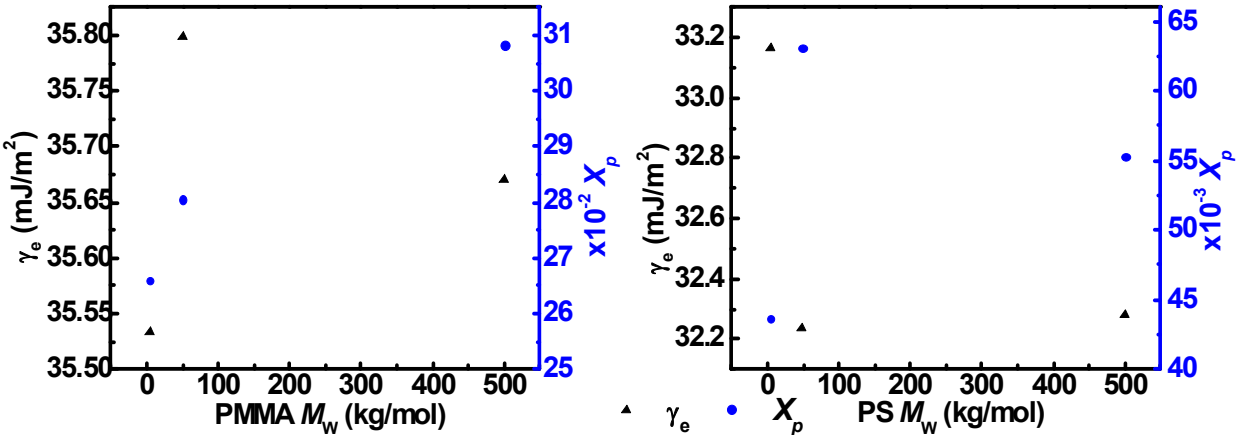

Figure S2. Estimated surface energy and surface polarity for PMMA (left) and PS (right) films of different M_w.

Film surface	$\theta_{a,water}$ ± sd (°)	$\theta_{a,\ MEG}$ ± sd (°)	$\theta_{a,\ DMSO}$ ± sd (°)	σ_S^D (mJ/m^2)	σ_S^P (mJ/m^2)	γ_e (mJ/m^2)	χ_p
PMMA1	74.4 ± 0.4	49.5 ± 0.1	33.6 ± 1.1	26.1	9.5	35.53	0.27
PMMA2	73.6 ± 1.1	48.6 ± 0.4	33.4± 0.1	25.8	10.0	35.80	0.28
PMMA3	72.5 ± 0.6	50.1 ± 0.1	32.5 ± 0.1	24.7	11.0	35.67	0.31
PS1	91.5 ± 0.7	66.3 ± 0.1	40.8 ± 3.6	31.7	1.4	33.17	0.04
PS2	89.9 ± 1.1	66.4 ± 0.4	40.7 ± 0.1	30.2	2.0	32.24	0.06
PS3	90.8 ± 0.6	66.9 ± 0.5	41.3 ± 0.8	30.5	1.8	32.28	0.06
F8BT	97.4 ± 4.9	73.8 ± 0.6	65.7 ± 1.5	19.8	2.3	22.18	0.11

Table S1. Film surface wettability properties of polymeric dielectrics and organic semiconductor employed in this study with contact angle on water, ethylene glycol and DMSO, the corresponding surface energy and surface polarity were estimated using the mean values by employing Owens and Wendt method.

2. Morphological characterization

The morphology of the PMMA and PS for all the different molecular weights exhibited amorphous nature (Figure S3 a-f). Veeco instruments Dimension 3100 ambient atomic force microscope (AFM) was employed in tapping mode (TM) was employed to collect the images of the morphology of the semiconductor and dielectric films. Table S2 collects the root mean square roughness of the thin polymeric dielectric films.

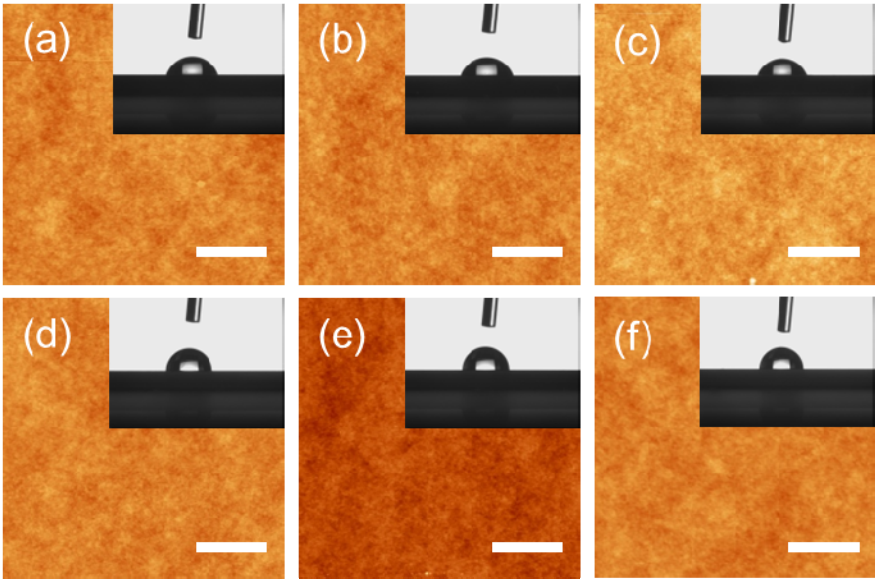

Figure S3. 2x2 μm^2 TM-AFM height images of polymer dielectric films a) PMMA1, b) PMMA2, c) PMMA3, d) PS1, e) PS2 and f) PS3. White scale bar represents 500 nm, and Z-scale = 8.93 nm. The inset shows the optical images of the static aqueous contact angle on the dielectric surface.

Film surface	RMS roughness (nm)
PMMA 1	0.37
PMMA 2	0.36
PMMA 3	0.41
PS 1	0.34
PS 2	0.35
PS 3	0.31
F8BT	0.41

Table S2. Root mean square roughness values of dielectric and semiconductor film surface. For the PMMA and PS dielectrics the RMS roughness was estimated from an area of 2x2 μm^2 while it was 1x1 μm^2 F8BT film.

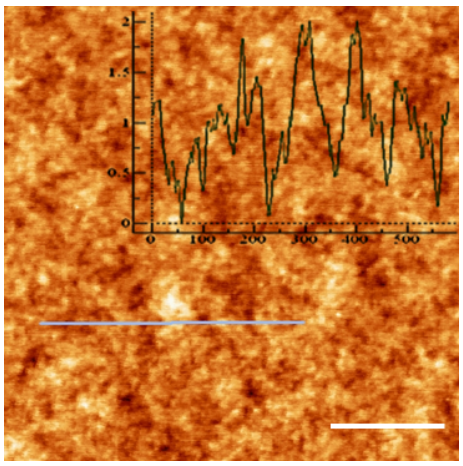

Figure S4. 1x1 μm^2 area, height image of spin casted F8BT film on Si/SiO_2 substrate. Inset shows the height profile image of the selected grey region. Z-scale is 3.5 nm and white scale bar denotes 250 nm.

3. Dielectric breakdown strength

The dielectric breakdown strength measurements for all the polymeric dielectrics were performed on metal-insulator-metal (MIM) configuration. The MIM structures were formed by first casting respective dielectrics from solution onto Si/SiO_2 substrates coated with a layer of Au (~ 50 nm) to form the bottom electrode plate following which the top electrode plate was fabricated by sputtering Au ~ 30 nm using Emitech K575X sputter coater. The breakdown strength was evaluated using the relation $E = V/d$, where E is electric field strength, V the applied potential between the electrodes and d is the thickness of the dielectric layer. Figure S5 shows the maximum current density which the dielectric could withstand before breaking down under the application of electric field. All the dielectric employed in this study exhibited fairly good breakdown voltage strength ~ >1 MV/cm.

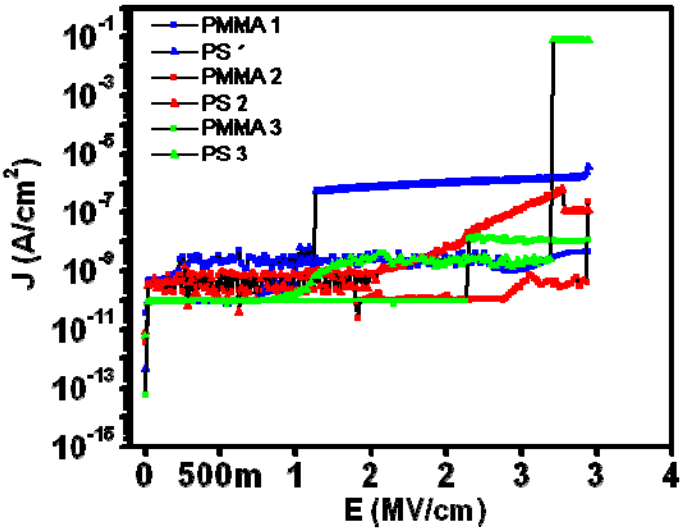

Figure S5. Plot showing the magnitude of electric field which the polymeric dielectrics could withstand before occurrence of break down.

4. Work function of source-drain electrodes

We recorded the work function of the electrodes by means of ambient Ultraviolet spectrophotometer (UPS) from Riken Keiki Co Ltd model AC-2.

For work function measurements Cr-Au back contact of 5 nm + 30 nm were evaporated onto Si/SiO_2 substrates in thermal evaporator (Plassys MEB 300) at a base pressure of ~10^{-6} mbar. Then the substrates were transferred though within ~120 s to the sample stage of the ambient UPS and work function values were recorded immediately. Figure S6 shows the work function of Au which is estimated by the minimum threshold energy required for photoelectron emission to commence from the ground state.

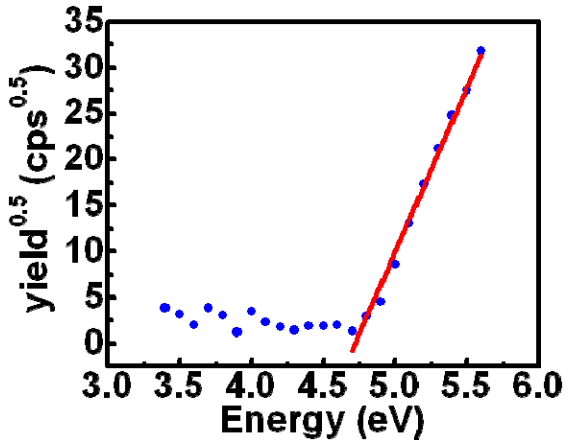

Figure S6. Work function of evaporated Au film estimated from the ratio of square root of photoelectron yield with respect to the energy.

The work function of Au amounts 4.82 ± 0.03 eV, as determined by averaging 6 different measurements.

The work function of Au with a chemisorbed SAM of 1-undecanethiol ($C_{11}H_{23}SH$), amounts ton to 4.4 ± 0.02 eV.

5. Ionization energy of organic semiconductor

We recorded the ionization energy of our F8BT semiconductor film by means of ambient Ultraviolet spectrophotometer (UPS) from Riken Keiki Co Ltd model AC-2.

Firstly ~120 µl of 6 mg×ml^{-1}F8BT solution in $CHCl_3$ was drop casted onto a custom solution holder inside N_2 filled glovebox and the solvent was allowed to dry. The ionization energy (IE) gives the lowest energy required to create a hole in the highest occupied molecular orbital (HOMO) upon the photoemission of an electron.[2] The IE was estimated from the photo electron yield *vs* energy plot (Fig. S7). IE value of 5.92 ± 0.02 eV was estimated from 10 individual measurements on different spots of the F8BT film.

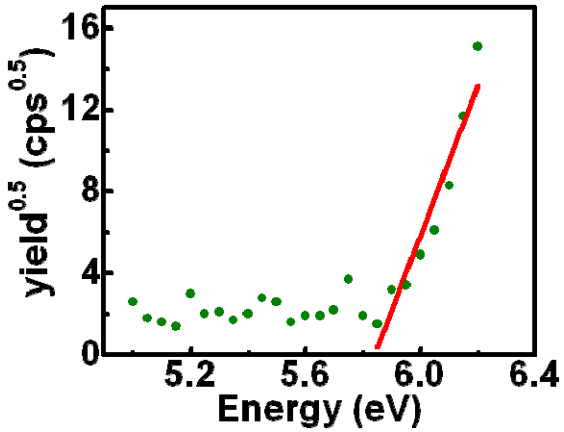

Figure S7. Ionization energy of drop casted F8BT film estimated from the ratio of square root of photoelectron yield as a function of energy.

6. Dynamic bias stress transfer characteristics

We used Keithley 2636A dual channel electrometer. For testing the devices under the influence of continuous dynamic I_{DS}-V_{GS} characteristic sweeps we swept the gate electrode from 0 V → -80 V → 0 V at 2 V steps for p-type device operation and 0 V → +80 V → 0 V at 2 V steps for n-type device operation keeping the V_{DS} constant at ± 40 V or ± 60 V respectively depending on the type of majority charge carrier. Shown in Fig. S8 are the transfer characteristics for transistor operating in electron and hole enhancement mode with PMMA1 as the gate dielectric. The entire

characterization was performed inside a N_2 filled glovebox. Custom in-house developed code was used to trigger, source the electrometer and read out the measured data following the logical sequence of steps.

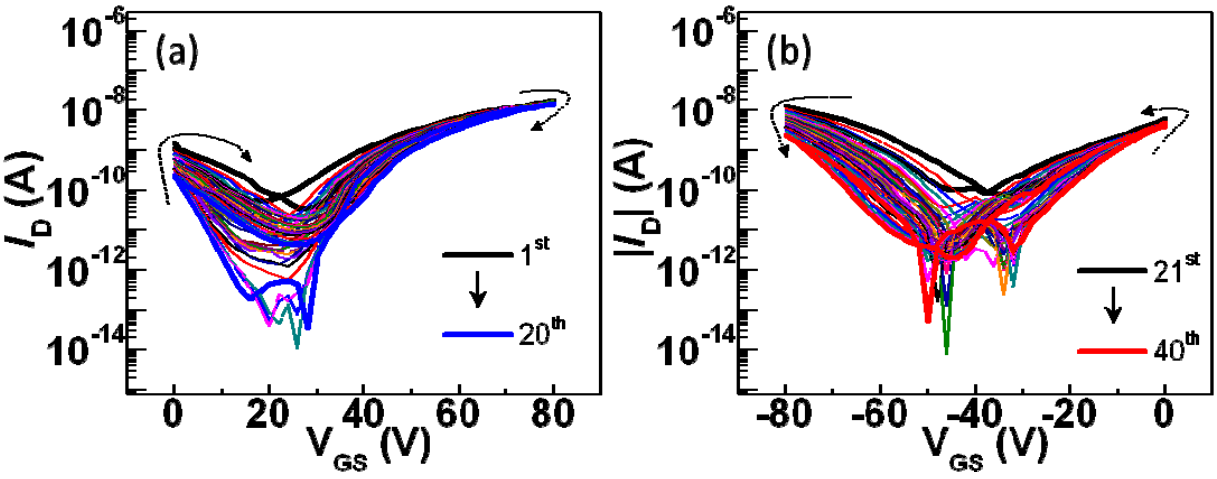

Figure S8. Transfer characteristics (semi-log I_D *vs.* V_{GS} plots) of device based on PMMA1 dielectric indicating 20 cycles for both (a) n-type (left panel) and (b) p-type (right panel) operation, the V_{DS} was fixed at ±60 V depending of the majority carrier and the device channel length-to-width ratio was 125. Curved dashed arrows represent the direction of the gate potential sweep.

Polymer dielectric	V_{on} 1st (V)[a]	V_{on} 20th (V)[b]	S 1st (V/dec)[c]	S 20th (V/dec)[d]	ΔS (V/dec)[e]	$I_{D,max}$ 1st x10^{-8} (A) [f]	$I_{D,max}$ 20th x10^{-8} (A) [g]	$\Delta I_{D,max}/I_{D,max1}$ st % [h]	I_{on}/I_{off} 1st (log_{10})[i]	I_{on}/I_{off} 20th (log_{10})[j]
PMMA 1	20	30	10.6	11.7	1.1	1.8	1.5	-17.84	2	5
PMMA 2	26	24	10.3	12.2	1.9	2.6	2.2	-12.46	2	4
PMMA 3	28	36	10.4	11.6	1.1	2.3	1.9	-13.91	3	4
PS 1	24	16	9.2	9.6	0.4	17.5	14.5	-17.17	2	3
PS 2	40	48	10.1	10.2	0.1	1.4	1.2	-18.62	2	2
PS 3	50	56	9.7	9.9	0.1	1.5	1.1	-27.47	2	2
PMMA 1	-36	-52	10.5	11.6	1.1	-1.30	-0.24	-81.4	2	5
PMMA 2	-32	-42	10.0	12.0	2.0	-2.19	-0.40	-81.5	2	4
PMMA 3	-34	-50	11.0	12.3	1.3	-0.50	-0.03	-94.7	2	2
PS 1	-30	-24	8.6	9.7	1.1	-62.40	-19.98	-68.0	2	3
PS 2	-42	-56	10.2	10.5	0.3	-5.18	-0.97	-81.3	2	2
PS 3	-54	-60	10.2	10.9	0.7	-0.85	-0.05	-94.4	2	2

Table S3. TFT performance indicators under dynamic bias stress tests for ambipolar switching operation taken from forward I_D-V_{GS} trace with V_{DS} held at ±60 V, [a] V_{on} at 1st cycle. [b] V_{on} at 20th cycle. [c] Subthreshold slope in 1st cycle. [d] S in 20th cycle. [e] Change in S. [f] $I_{DS,max}$ 1st cycle collected when V_{GS}= 80 V for electron (V_{GS}= -80 V for hole). [g] $I_{D,max}$ 20th cycle collected when V_{GS}= 80 V for electron (V_{GS}= -80 V for hole). [h] Change in $I_{D,max}$ from 1st to 20th switching cycle collected when V_{GS}= 80 V for electron (V_{GS} = -80 V for hole). [i] I_{on}/I_{off} at 1st cycle. [j] I_{on}/I_{off} at 20th cycle.

7. Transistor Electrical characterization

The electrical characterization of OTFTs was recorded by means of a Keithley 2636A source measure unit (SMU). For each of the device measured firstly the n-type channel was probed followed by the p-type channel by collecting the transfer characteristic curves I_D-V_{GS} followed by the output curves (I_D *vs.* V_{DS}). Triaxial cable shielding was utilized to minimize signal losses. To

ensure reasonable uniformity during electrical characterization from one batch to another all measurements were carried out in the dark inside a N_2 filled glovebox. Table S4 collects the yield among the total number of devices measure of different channel lengths (L) characterized while Table 5 reports the measured V_T and V_{ON} values which appear in Fig. 4 in the main text.

Dielectric in OTFT	Out of 16	yield (%)
PMMA1	13	81.25
PMMA2	14	87.5
PMMA3	13	81.25
PS1	10	62.5
PS2	16	100
PS3	11	68.75

Table S4. Yield of the devices after electrical characterization.

Polymer dielectric	$V_{T,e^-} \pm \sigma$ (V)	$V_{ON,e^-} \pm \sigma$ (V)	$V_{T,h^+} \pm \sigma$ (V)	$V_{ON,h^+} \pm \sigma$ (V)
PMMA1	24.2 ± 5.6	27.5 ± 9.8	-38.9 ± 6.4	-41.5 ± 8.1
PMMA2	28.6 ± 1.0	36 ± 5.2	-31.7 ± 5.3	-36 ± 4.9
PMMA3	33.5 ± 4.0	38.7 ± 4.6	-35.1 ± 9.4	-38 ± 7.2
PS1	34.7 ± 16 .2	52 ± 2.8	-42.7 ± 3.9	-37 ± 9.9
PS2	41.9 ± 3.4	39 ± 2.6	-42.2 ± 6.0	-28 ± 4
PS3	39.8 ± 4.3	40 ± 9.1	-33.4 ± 6.9	-28.5 ± 10.1

Table S5. Threshold and turn-on voltage of the devices operating in *n* and *p*-channel mode

8. References and notes

[1] D. K. Owens, R. C. Wendt, J. Appl. Polym. Sci. 1969, 13, 1741.
[2] I. Hill, A. Kahn, Z. Soos, R. Pascal Jr, Chem. Phys. Lett. 2000, 327, 181.